Reaction Kinetics, Mechanisms and Catalysis (2021) 133:713–728
https://doi.org/10.1007/s11144-021-02037-1

Hydrogen production from decalin over silica-supported platinum catalysts: a kinetic and thermodynamic study

Evgeniya A. Martynenko[1] · **Sergei V. Vostrikov**[1] · **Aleksey A. Pimerzin**[1]

Received: 18 June 2021 / Accepted: 22 July 2021 / Published online: 27 July 2021
© Akadémiai Kiadó, Budapest, Hungary 2021

Abstract

Decalin dehydrogenation for efficient hydrogen production over platinum catalysts supported on different types of silica was studied. The catalytic properties of the prepared catalysts were tested under conditions of a flow installation. It was found that from a thermodynamic point of view, high temperatures will favor dehydrogenation, and low temperatures will favor the isomerization of *cis*-decalin to *trans*-decalin. It negatively affects the rate of decalin dehydrogenation; therefore, kinetic control is required. It was shown that the catalysts supported on mesoporous silica MCM-48 and SBA-15 showed a significantly higher catalytic activity during decalin dehydrogenation compared to catalysts supported on amorphous SiO_2. The high surface area and small pore size of these supports positively affect Pt particles' dispersion and result in the production of high-active catalysts for dehydrogenation of decalin to naphthalene. The maximum decalin conversion was observed over the 2% Pt/MCM-48 catalyst at a pressure of 0.5 MPa, a 325 °C temperature, and an LHSV of 20 h^{-1}. This study provides a rationale for the proper support selection for efficient utilization of decalin as a LOHC.

Graphic abstract

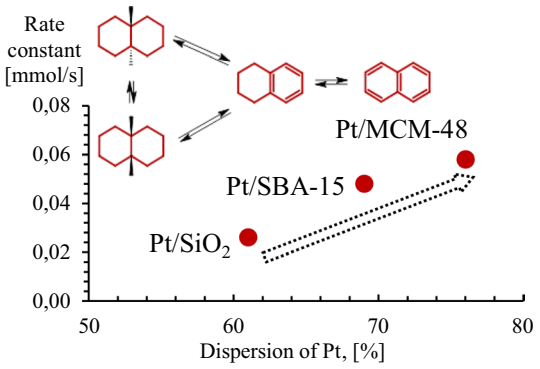

Extended author information available on the last page of the article

Keywords Hydrogen · Decalin · Dehydrogenation · Pt catalysts · Kinetic · Thermodynamic

Introduction

Hydrogen is one of the most promising energy carriers nowadays due to its high energy density and low pollutant effects in its use [1]. However, it is important to solve hydrogen storage for the practical application of the hydrogen energy system in the near future. Several strategies have been proposed for hydrogen storage, such as storing hydrogen at high pressure or cryogenic temperature, but it still leaves a question in logistics and safety. Storage systems based on metal hydrides are characterized by a high theoretical capacity of hydrogen, but the hydrogen generation from the hydrides still requires further research [2, 3].

Another high-potential technology for hydrogen storage is the reverse storage of hydrogen through its chemical bonding in molecules of organic compounds (i.e., hydrogenation and dehydrogenation). According to this concept, a hydrogen-depleted liquid organic hydrogen carrier (LOHC) molecule is hydrogenated in a place where there is an excess of cheap hydrogen. The hydrogen-enriched molecule can then be stored for a long time or transported using current infrastructure and, if necessary, be released at energy consumption [4, 5].

LOHCs are high boiling organic molecules that can be easily and reversibly hydrogenated and dehydrogenated during the catalytic processes. There are several requirements for LOHC systems: thermal stability, a suitable melting point, favorable thermodynamics of dehydrogenation, wide availability, low toxicity, and a reasonable price [6]. Various kinds of LOHC materials have been proposed and investigated. The first studied system for the technology of LOHC was based on a toluene/methylcyclohexane pair [7]; then many other paired systems were studied, for example, biphenyl/bicyclohexyl [8], dibenzyltoluene/perhydro-dibenzyltoluene [9], N-heterocyclic hydrocarbons [10], and many others. Polycyclic and condensed compounds are promising organic substrates-carriers of H_2 for LOHC systems since they have some advantages: low volatility (compared with toluene) and higher stability (compared with heterocycles like N-ethylcarbazole). Decalin is often considered in the literature as a promising candidate among polycyclic aromatic compounds [11, 12] because it meets most of the requirements for LOHC. The theoretical amount of hydrogen obtained from one mole of decalin is 5 mol of H_2, corresponding to 7.3 wt%. An additional advantage of decalin dehydrogenation is the final product of the dehydrogenation of decalin is naphthalene, which can be easily converted back to decalin by catalytic hydrogenation using a well-studied industrial process.

The catalysts used in LOHC systems significantly affect the operational characteristics of such systems, especially the rate and conditions of the dehydrogenation process. Therefore, selecting an efficient catalyst able to withstand repeated cycles of hydrogenation/dehydrogenation is also in the spotlight. Platinum is most often used as an active phase of catalysts for the decalin dehydrogenation reaction [11–17]; less commonly is used nickel [18, 19] or palladium [20–22]. It is well known that the type of carrier has a significant impact on the properties of the

catalyst: the properties of the support directly affect its interaction with the metal, the dispersion of the active component, which largely determines the catalyst activity, its selectivity, and its productivity. Alumina and activated carbon are the most used catalyst supports for dehydrogenation. Studies show that hydrogenation/dehydrogenation occurs at metal sites, while cycle opening, cracking, and isomerization reactions (including *cis*-decalin to *trans*-decalin isomerization) occur at acidic sites [23]. From this point of view, it seems attractive to use silica with low acidity as support. Besides the nature of the support, the support structure can also affect the activity of the catalyst. In our previous study [24], it was already reported that Pt catalysts supported on mesoporous silica MCM-48 and SBA-15 are more active for decalin dehydrogenation than catalysts supported on traditional SiO_2 and Al_2O_3. These mesostructured materials with high surface area, ordered pore structure, and uniform pore size distribution has attracted considerable attention as catalyst support. Moreover, in work [25] is shown that metal nanoparticles confined in well-defined mesoporous materials showed unusual thermal stability, which is essential to their applications, especially for high-temperature catalytic reactions.

The present research is aimed at investigates the activity of the Pt/SiO_2, Pt/SBA-15, and Pt/MCM-48 catalysts in decalin dehydrogenation and a more detailed study of the kinetic and thermodynamic characteristics of this reaction. The obtained results provide useful data concerning the silica type's role as a support for Pt catalysts for dehydrogenation reactions.

Experimental section

Support and catalyst preparation

A commercial sample of silica (CAS 7631-86-9, Sigma-Aldrich), and the mesoporous silica SBA-15 and MCM-48 (were synthesized ourselves) were used as supports.

SBA-15 was synthesized according to a typical procedure described earlier by Zhao et al. [26] using a Pluronic P123 (CAS 9003-11-6, Sigma-Aldrich) copolymer as a structure-directing agent and tetraethyl orthosilicate TEOS (CAS 78-10-4, Sigma-Aldrich, purity 98%) as a silica source. Pluronic P123 (4 g) was dissolved in 30 g of water and 120 g 2 M HCl solution with stirring at 25 °C. Then 8.50 g of TEOS was added into that solution with stirring at 35 °C for 20 h. Then the mixture was aged at 80 °C overnight without stirring. The solid product was recovered by filtration, washed, and air-dried at room temperature. The calcination was carried out by the slowly increasing temperature from the room temperature to 500 °C in 8 h and heating at 500 °C for 6 h. The nominal molar composition used in the synthesis was 1TEOS: 0.017P123: 5.95 HCl: 171H_2O.

MCM-48 was prepared by a room temperature synthesis described previously [27]. A 5.2 g of cetyltrimethylammonium bromide CTAB (CAS 57-09-0, Sigma-Aldrich, purity ≥ 98%) was dissolved in 240 mL of deionized water and 100 mL of ethanol (CAS 64-17-5, purity 95%). After the solution became clear, 24 mL of aqueous ammonia (CAS 1336-21-6, Vekton, 25 wt%) was added to the solution. The

solution was stirred for 10 min (450 rpm), and 7.2 g of TEOS was added under vigorous stirring. The gel's molar composition was 1 M TEOS:12.5 M NH_3:54 M EtOH:0.4 M template:417 M H_2O. After being stirred for 15 h respective at room temperature, the solid product was recovered by filtration, washed, and dried at room temperature during the night. To remove the template the dried material was calcined at 560 °C for 6 h.

Catalysts were prepared by incipient wetness impregnation technique. 2 or 6 wt% of platinum was loaded from the aqueous solution of chloroplatinic acid H_2PtCl_6 (CAS 26023-84-7). The impregnated samples were dried at 60 °C (2 h), 120 °C (6 h), and calcined at 450 °C in air for 1 h (with a heating rate of 1 °C/min). Catalysts reduction was carried out in excess of pure hydrogen at 400 °C for 2 h in the chemical reactor, in which the catalytic test of the prepared sample was then carried out.

Support and catalyst characterization

The textural characteristics of the synthesized supports and catalysts were studied by N_2 physisorption using a Quantochrome Autosorb-1 system. Specific surface areas were calculated by the Brunauer–Emmett–Teller (BET) method (S_{BET}), the total pore volume (V_p) was determined by nitrogen adsorption at a relative pressure $P/P^0 = 0.98$, and the pore size distribution curve came from the analysis of the desorption branch of the isotherm from by the BJH (Barrett–Joyner–Halenda) method.

The reduced catalysts were studied by high-resolution transmission electron microscopy (HRTEM) using a Tecnai G2 20 electron microscope with a LaB6 cathode, a resolution of 0.14 nm, and an accelerating voltage of 200 kV.

Catalytic activity tests in decalin dehydrogenation

The commercially available decalin (Vekton, Russia) was used as a substrate. It contains *cis*-, *trans*-isomers, and tetralin in 83.7 wt%, 8 wt%, and 8.3 wt%.

Catalytic decalin dehydrogenation was carried out on supported Pt catalysts in a laboratory fixed-bed tubular reactor at temperatures of 300–335 °C, a pressure of 0.5 MPa, a liquid hourly space velocity of 1–120 h^{-1}, and an H_2/feed ratio of 500 nL/L. A process flow diagram and the configuration of each continuous reactor are shown in Fig. S1 in supplementary material. Mass flow controllers controlled the gas feeds, and a reciprocating pump fed the liquid. The reaction temperature was controlled by the electric furnace and was measured by thermocouples in the middle of the catalytic bed. Into the isothermal zone of the reactor 0.37–4 cm^3 of catalyst (fraction 0.25–0.5 mm) and silicon carbide (the same size) were loaded in the ratio of 1/1. In a typical run, the solution of decalin in n-heptane (1 wt%) was used as a feed mixture. Product mixtures were cooled and separated at a vapor–liquid separator at room temperature. The reaction was followed by withdrawing of samples (at least once per hour) and analyzing them in the Crystal-2000M gas–liquid chromatograph equipped with a flame ionization detector (Chromatek, Russia) and capillary column ZB-35 (30 m × 0.25 mm × 0.25 μm film thickness, 35% phenyl and 65%

dimethylpolysiloxane); carrier gas—helium. To corroborate product identification the reaction mixture was analyzed on GCMS-QP2010 Ultra instrument (Shimadzu).

Decalin conversion was calculated using the equation:

$$X_{0D} = \frac{C_{0D} - C_D}{C_{0D}} \times 100, \tag{1}$$

where C_{0D} is the initial concentration of *cis*- and *trans*-decalins, mol/L; C_D is the concentration of *cis*- and *trans*-decalins in the reaction mixture, mol/L.

The selectivity of the dehydrogenation reaction was calculated using the equation:

$$S_i = \frac{C_i}{C_{\sum i}} \times 100, \tag{2}$$

where C_i and $C_{\Sigma i}$ are the concentration of the individual products and all the reaction products, mol/L.

According to [11, 12, 28], a Langmuir-type rate equation (Eq. 3) has been successfully applied to describe the catalytic dehydrogenation of decalin:

$$r = \frac{k}{1 + K \cdot C_N}, \tag{3}$$

where r is the hydrogen evolution rate, mmol/s, k is the reaction rate constant, mmol/s, C_N is the naphthalene molar concentration, (mmol/mL), K is the retardation constant, mL/mmol.

The dispersion of platinum on the catalyst surface was calculated from the total metal loading and the average particle size obtained by HR TEM analysis, assuming that the platinum particles are spherical shape.

$$D = \frac{[\mathrm{Pt}]_{surf}}{[\mathrm{Pt}]_{tot}} \times 100\%, \tag{4}$$

where $[\mathrm{Pt}]_{surf}$ is the amount of surface Pt atoms of the metal nanoparticles, evaluated from average particles size; $[\mathrm{Pt}]_{tot}$ is the total amount of platinum loaded for the corresponding catalyst, mol%.

Results and discussion

Characterization of supports and catalysts

The textural properties of the used supports and catalysts are shown in Table 1. The characteristics of synthesized mesoporous materials are consistent with previously published results [29–31]. Mesoporous silica SBA-15 and MCM-48 have a higher specific surface area and narrow pore size distribution compared to SiO_2. For all catalysts, it is possible to observe a decrease in the values of pore size, pore-volume, and total area in relation to the support.

Table 1 Textural and structural characteristics of supports and prepared catalysts

Sample	S_{BET} [m^2/g]	V_P [cm^3/g]	D_P [nm]	Average particle size [nm]	Dispersion [%]
SiO_2	360	0.99	9.5	–	–
SBA-15	849	0.86	5.6	–	–
MCM-48	1561	0.64	2.7	–	–
2 Pt/SiO_2	339	0.93	8.3	2.5	61
6 Pt/SiO_2	344	0.97	8.6	3.1	49
2 Pt/SBA-15	634	0.61	5.3	2.2	69
2 Pt/MCM-48	1348	0.55	2.6	2.0	76

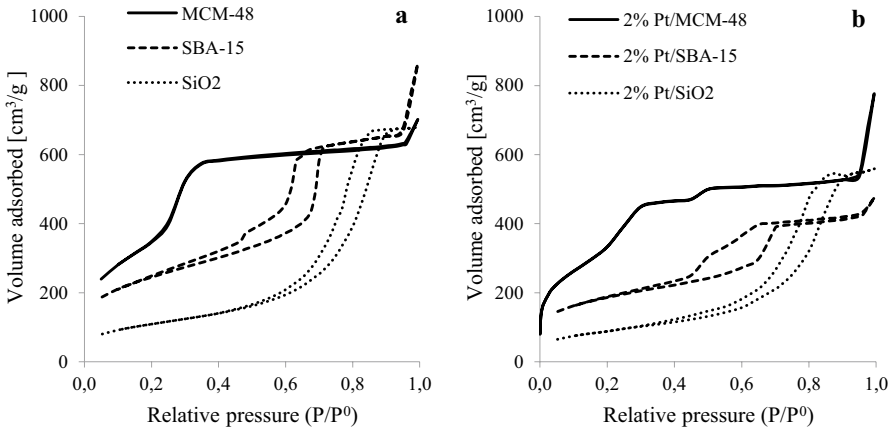

Fig. 1 Nitrogen adsorption isotherms of the supports (**a**) and catalysts (**b**)

Fig. 1 shows nitrogen adsorption–desorption isotherms of supports and catalysts. The MCM-48 displays a type IV isotherms in the IUPAC classification and a sharp inflection on the range of $P/P^0 = 0.2–0.4$, which occurs due to capillary condensation of nitrogen in the mesoporous [32]. For Pt/MCM-48, a progressive decrease in the amount of adsorbed nitrogen and mesopore volume was observed with the impregnation of Pt species on the surface. This decrease, in general, can be related to the deposition of Pt nanoparticles inside of the MCM-48 pores and also due to partial loss of structural ordering of the mesoporous channels [33].

SBA-15 and Pt/SBA-15 showed a type IV isotherm with an H1 hysteresis loop characteristic of a well-formed SBA-15 structure with cylindrical pore channels, with a small pore difference size. Impregnation of Pt species on the surface produced some changes in the shape of the hysteresis loop at relative pressures $P/P^0 = 0.4–0.7$ and decreased surface area and pore volume. It can be due to the deposition of the impregnated Pt species inside the SBA-15 support mesopores, as in the case of MCM-48.

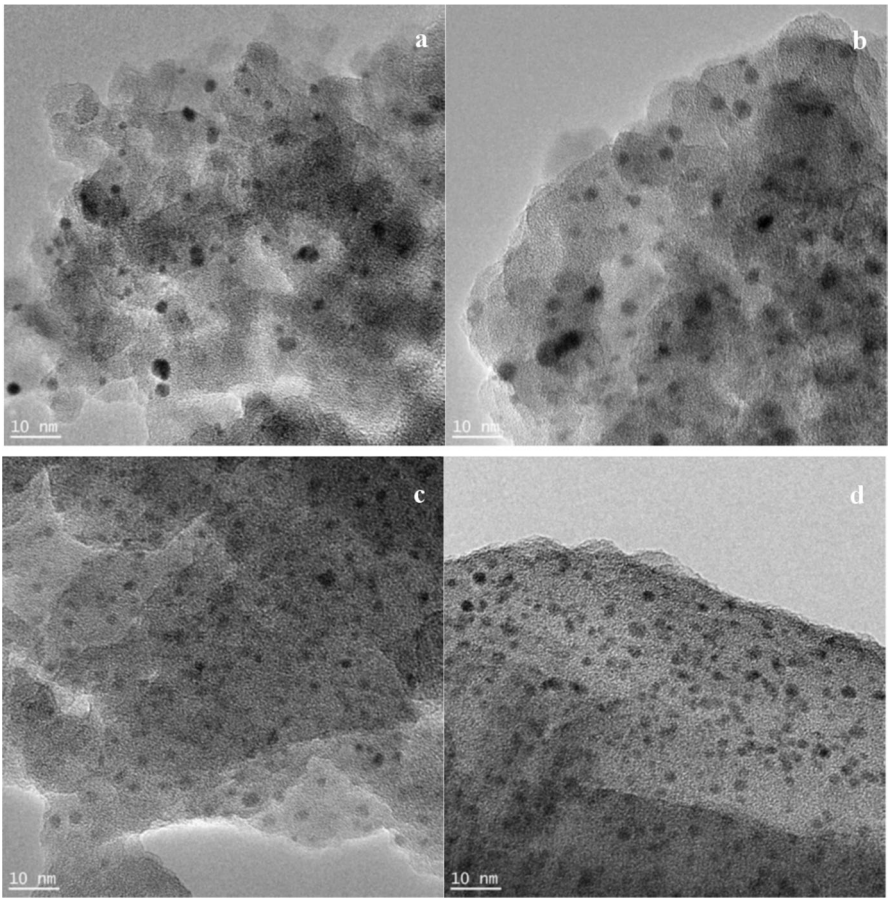

Fig. 2 TEM images of synthesized catalysts. **a** 6% Pt/SiO_2, **b** 2% Pt/SiO_2, **c** 2% Pt/SBA-15, **d** 2% Pt/MCM-48

Insight into the average particle size and the reduced Pt species' dispersion was made by high-resolution transmission electron microscopy. Fig. 2 shows the obtained images of the catalysts. In the micrograph of all catalysts, a considerable number of metallic Pt particles can be seen on the support's external surface. The size of particles for catalysts supported on amorphous SiO_2 did not exceed 3 nm, as determined by TEM analysis. Catalysts supported on mesoporous silica SBA-15 and MCM-48 were characterized by smaller particle size and correspondingly greater dispersion compared to catalysts on SiO_2 (Table 1). The average Pt particle size values determined by TEM were used to reveal the structure sensitivity in decalin dehydrogenation. Dispersion of metal was calculated on the basis of TEM data using an approximation from [34].

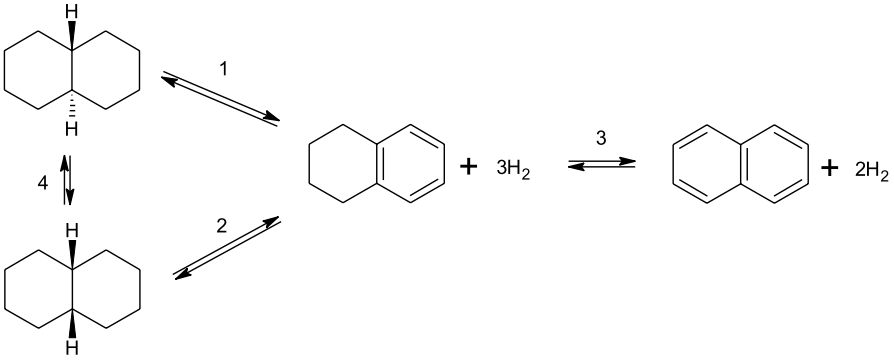

Scheme 1 Dehydrogenation of decalin to tetralin and naphthalene

Catalytic activity in the dehydrogenation of decalin

The dehydrogenation reaction of decalin (a mixture of *cis*- and *trans*-isomers) is shown in Scheme 1. The reaction of decalin dehydrogenation includes several simultaneous reactions: the formation of tetralin from *trans*- (1) and *cis*-decalin (2), the conversion of tetralin to naphthalene (3), and isomerization of *cis*- and *trans*-decalins (4).

Kalenchuk et al. [15] published a theoretical study on the chemical equilibrium of the decalin dehydrogenation reaction. It was shown that for both *cis*- and *trans*-decalin, the temperature dependencies of equilibrium concentrations of dehydrogenation products on temperature are entirely identical. However, the same values of equilibrium concentrations in the dehydrogenation of *trans*-isomer are reached at higher temperatures than in dehydrogenation of *cis*-decalin, which indicates a lower rate of *trans*-decalin dehydrogenation.

The first tested catalyst 6% Pt/SiO_2 showed high activity in the dehydrogenation reaction; however, at the increase of liquid hourly space velocity (LHSV) from 1 to 30 h^{-1}, the reaction mixture's composition remained almost the same (Fig. 3). Replacing the feed mixture with a solution of decalin (1 wt%) and naphthalene (1 wt%) in heptane and increasing the LHSV to 60 h^{-1} did not have any significant effect on the composition of the reaction mixture (white symbols in Fig. 3). It is evident that the catalyst 6% Pt/SiO_2 ensures the achievement of chemical equilibrium at relatively low values of LHSV under experimental conditions. This catalyst's experimental data made it possible to calculate the thermodynamic and kinetic parameters of the decalin dehydrogenation reaction.

Equilibrium constants for decalin dehydrogenation were calculated using experimental data for every step of dehydrogenation (1–4) in the temperature range 300–335 °C, and the pressure range 0.5–2 MPa. The obtained correlations of the equilibrium constants with temperature make it possible to calculate the

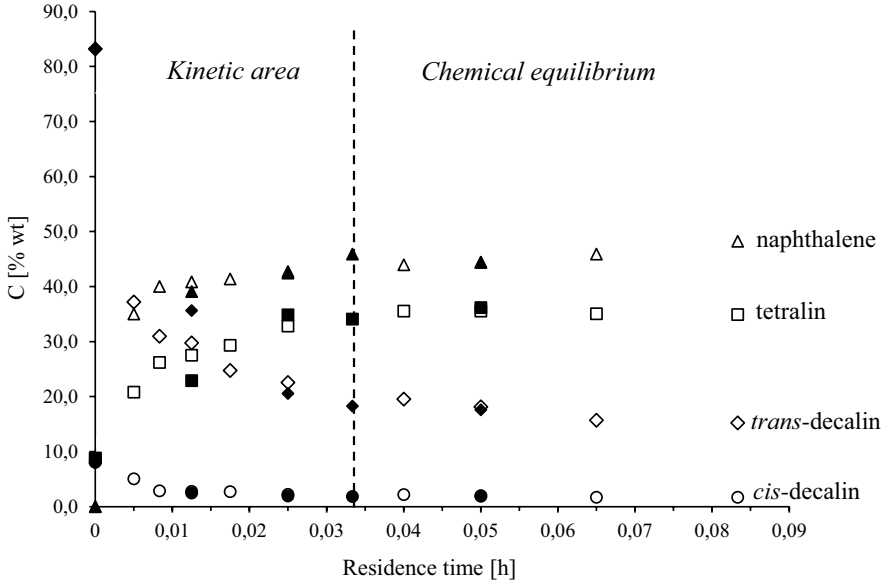

Fig. 3 The concentration of decalin and products of its dehydrogenation as a function of residence time; 6% Pt/SiO_2, 0.5 MPa, 325 °C; black symbols—for a feed mixture of decalin in heptane; white symbols—for a feed mixture of decalin and naphthalene in heptane

enthalpic and entropic effects of the reaction according to the isotherm equation of chemical equilibrium:

$$-RTln\left(K_p\right) = \Delta_r H_T - T \cdot \Delta_r S_T \tag{5}$$

From which

$$ln\left(K_p\right) = \frac{-\Delta_r H_T}{R} \cdot \frac{1}{T} + \frac{\Delta_r S_T}{R}, \tag{6}$$

where R is the gas constant 8.314472, kJ/(mol K); K_p is the equilibrium constant in the gaseous phase; T is temperature, K; $\Delta_r H_T$ is the enthalpy of the reaction, J/mol; $\Delta_r S_T$ is the entropy of the reaction, J/(mol K). Equilibrium constants and reaction enthalpies are shown in Table 2.

The obtained results related to the equilibrium constants and the enthalpies indicate that the reverse reactions play a significant role in the decalin dehydrogenation

Table 2 Equilibrium constants and enthalpies of decalin dehydrogenation steps

Reaction	K_p at 300 °C	$\Delta_r H_T$ [kJ/mol$_{H2}$]
trans-Decalin ↔ Tetraline + $3H_2$	18.7 ± 1.9	67.3 ± 1.9
cis-Decalin ↔ Tetraline + 3 H_2	168.6 ± 39.9	59.5 ± 2.8
Tetraline ↔ Naphtalene + 2 H_2	5.1 ± 0.6	63.4 ± 1.9
trans-Decalin ↔ *cis*-Decalin	0.12 ± 0.01	15.3 ± 1.0

reaction. The equilibrium constants at 300 °C for isomerization of *trans*-decalin into *cis*-decalin and reverse reactions were 0.12 and 9.1, respectively, which consistent with the results published in other studies [15, 35] and confirms that isomerization of *cis*- to *trans*-decalin is more likely than reverse reaction. The equilibrium constants at 300 °C for the reactions of dehydrogenation of *trans*-decalin to tetralin, *cis*-decalin to tetralin, and tetralin to naphthalene were 18.7, 168.6, and 5.1, which confirms the easier dehydrogenation of *cis*-decalin compared to *trans*-isomer.

The dependence of the equilibrium constant on temperature shows that the equilibrium constants of all reactions occurring during the dehydrogenation of decalin increase with increasing temperature. Thus, with an increase in the temperature, the less active *trans*-isomer is converted into the more active *cis*-decalin, which positively affects the rate of decalin dehydrogenation. A decrease in temperature under chemical equilibrium conditions will favor the isomerization of *cis*-decalin to *trans*-decalin. Therefore, hydrogen production from decalin requires kinetic control.

The conversion of *trans*-(a) and *cis*-decalin (b) as a function of the residence time (1/LHSV, h) over 6% Pt/SiO_2 in the temperature range 300–325 °C is shown in Fig. 4. It can be seen that the conversion of *trans*-decalin increases with increasing residence time, and when the residence time is > 0.05 h (LHSV < 20 h^{-1}), the conversion is reduced to the equilibrium value. In the case of *cis*-decalin, at a residence time > 0.05 h the conversion decreases more rapidly compared to *trans* -decalin. As shown in the figure, the lower is the reaction temperature, the faster the conversion decreases. This result confirms that the *cis/trans*-isomerization equilibrium constant increases with decreasing temperature.

For catalyst 6% Pt/SiO_2 selectivity to the final product of dehydrogenation—naphthalene—increases with increasing temperature. Thus, as the temperature rises from 300 to 325 °C, the selectivity to naphthalene increases from 31 to 55%, and selectivity to tetralin decreases from 69 to 45%.

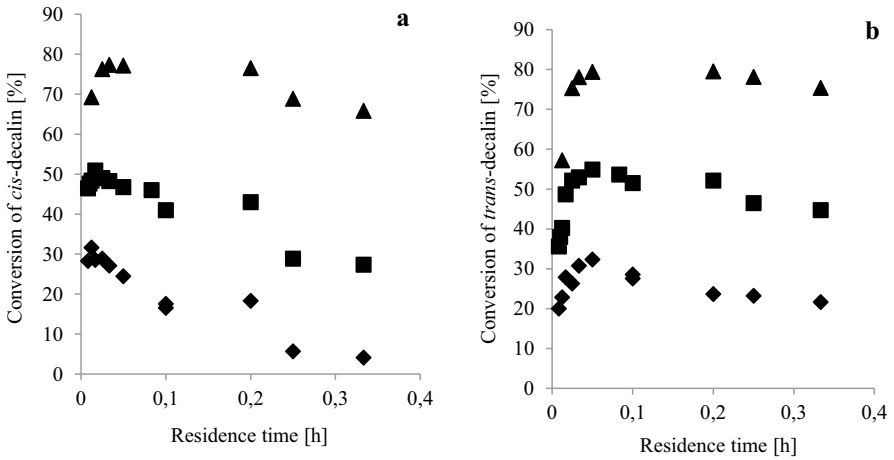

Fig. 4 *Cis*-decalin conversion (**a**), *trans*-decalin conversion (**b**) as a function of residence time; 6% Pt/SiO_2, 0.5 MPa, ◆—300 °C, ■—310 °C, ▲—325 °C, a feed mixture—decalin in heptane

The catalyst 2% Pt/SiO_2 showed lower activity than 6% Pt/SiO_2 under the same conditions, and as a result, it did not ensure the achievement of chemical equilibrium. For this catalyst, only the kinetic parameters were calculated. The dehydrogenation reaction's kinetics was calculated at a pressure of 0.5 MPa, H_2/feed ratio of 500 nL/L, varying LHSV from 1 to 120 h^{-1}, and temperature from 300 to 335 °C. The kinetic parameters for the 6% Pt/SiO_2 catalyst were studied at LHSV > 40 h^{-1} to avoid chemical equilibrium. Under experimental conditions, all the components' fugacity coefficients are close to one, which allows applying partial pressures and concentrations. Table 3 shows decalin conversion, selectivity to reaction products, rate constants k, and the naphthalene retardation constants K obtained for catalysts 6% Pt/SiO2 and 2% Pt/SiO_2. It was shown that decalin conversion decreases with an increase in the LHSV (with a decrease in the residence time). The selectivity to naphthalene and tetralin stays almost unchanged with an increase in the volumetric flow rate. A higher amount of platinum predictably leads to a higher catalyst activity; therefore, the highest decalin conversions and rate constants were observed for the 6% Pt/SiO_2 catalyst. The maximum decalin conversion value was about 75% at LHSV of 40 h^{-1}, a pressure of 0.5 MPa, and a temperature of 325 °C.

Activity tests of catalysts 2% Pt/SBA-15 and 2% Pt/MCM-48 showed that the use of mesoporous silicas with the same metal loading increases the catalytic activity compared with the catalyst 2% Pt/SiO_2. These data are consistent with the results

Table 3 Activity of silica-supported Pt catalysts in the dehydrogenation of decalin

t [°C]	LHSV [h^{-1}]	(*cis* + *trans*) Decalins conversion [%]	Selectivity to tetralin [%]	Selectivity to naphthalene [%]	$k \times 10^2$ [mmol/s]	K [mL/mmol]
6% Pt/SiO_2						
300	40	28	66	34	2.3	1.37
310	40	52	59	41	5.6	1.53
325	40	75	45	55	9.3	1.65
2% Pt/SiO_2						
300	20	19	71	29	0.5	1.35
310	20	35	61	39	1.1	1.42
325	20	59	44	56	2.6	1.61
335	20	68	33	67	4.0	1.65
2% Pt/SBA-15						
300	20	26	69	31	0.6	1.32
310	20	48	57	43	1.8	1.53
325	20	75	43	57	4.8	1.67
335	20	76	41	59	6.1	1.69
2% Pt/MCM-48						
300	20	40	61	39	1.3	1.45
310	20	62	49	51	2.5	1.60
325	20	85	36	64	5.8	1.72
335	20	86	31	69	8.1	1.74

obtained in our previous work [16] and indicating that mesoporous silicas, due to their textural characteristics, improve the dispersion of oxide and metal Pt nanoparticles on the surface of supports. The dehydrogenation reaction rapidly reaches chemical equilibrium, as in the case of 6% Pt/SiO_2 catalyst.

Table 3 shows decalin conversions' values, selectivity to reaction products, the overall rate constants, and retardation constants for Pt catalysts supported on SBA-15 and MCM-48. By comparing these two catalysts, it can be seen that at the almost similar decalin conversions (325 °C, LHSV 60 h^{-1}), the selectivity to naphthalene is higher for the Pt/MCM-48 catalyst. At the same time, at temperatures of 300–310 °C for both catalysts were observed almost the same distribution of reaction products and low selectivity for naphthalene. This is probably due to the fact that Pt catalysts are preferable in the conversion of decalin to tetralin, whereas Pd is preferable in the conversion of tetralin to naphthalene [22]. The reason for this difference in catalytic activity on Pd and Pt catalysts was the preference for the formation of adsorption modes during the sequential decomposition of hydrogen. The dependence of rate constants on the Pt dispersion is visualized in Fig. 5. It is evident that the rate constant in dehydrogenation gradually increases with Pt dispersion. Moreover, for catalysts supported on MCM-48, rate constant is approximately two times higher than for Pt/SiO_2. The obtained dependence indicates that the decalin dehydrogenation is structurally sensitive and the particle size affects the reaction kinetics.

The Arrhenius plots was used to determine the apparent activation energies for decalin dehydrogenation on all catalysts. This reaction's apparent activation energy in the temperature range from 300 to 335 °C is 180 ± 26 kJ/mol. This value is consistent with the literature data, according to which the activation energy for this type of reaction is on average 150–188 kJ/mol [36, 37].

Experimental data show that over catalyst 2% Pt/MCM-48 at a temperature of 325 °C, and an LHSV of 20 h^{-1}, the maximum decalin conversion was observed

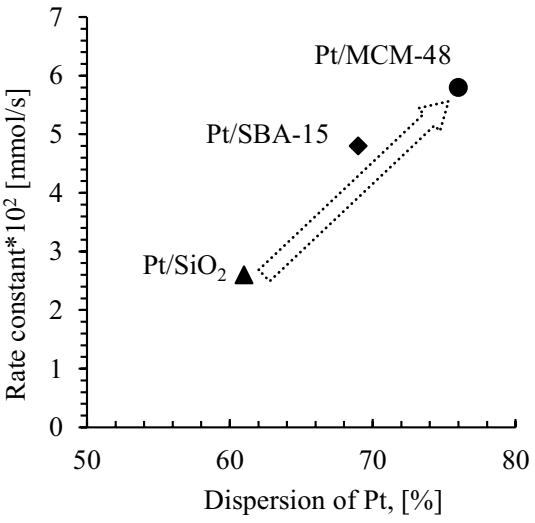

Fig. 5 Effect of Pt dispersion on the rate constants of decalin dehydrogenation for decalin dehydrogenation over Pt catalysts, 0.5 MPa, 325 °C, a feed mixture—decalin in heptane

without the formation of by-products. The decalin conversion under these conditions was 85%, and selectivity to naphthalene was about 60%. The maximum selectivity for naphthalene (74%) was observed under the same conditions at LHSV = 60 h^{-1}.

Conclusion

The kinetic and thermodynamic parameters of the decalin dehydrogenation reaction over Pt catalysts supported on different types of silica were investigated. The dehydrogenation of decalin includes four reversible reactions: in addition to the sequential dehydrogenation of decalin through tetralin to naphthalene, isomerization of the *cis–trans* isomers of decalin also occurs. It creates additional difficulties in implementing the process because the *cis*-isomer's activity significantly exceeds the activity of the *trans*-isomer in the dehydrogenation reaction. Under thermodynamic reaction control, the equilibrium constant of *cis*- into *trans*-decalin isomerization decreased with temperature. Consequently, high temperatures will favor dehydrogenation, and low temperatures will favor the isomerization of *cis*-decalin to *trans*-decalin. Therefore, hydrogen production from decalin requires kinetic control.

The catalysts supported on mesoporous silica SBA-15 and MCM-48 showed a significantly higher catalytic activity during dehydrogenation compared to the catalyst supported on amorphous SiO_2. The high surface area and small pore size of these supports have a positive effect on Pt particles' dispersion and result in the production of high-active catalysts for dehydrogenation of decalin to naphthalene. The maximum decalin conversion was observed over the 2% Pt/MCM-48 catalyst at a pressure of 0.5 MPa, a 325 °C temperature, and an LHSV of 20 h^{-1}. In this case, catalyst deactivation was not observed, as well as the formation of by-products. The obtained data can be used for the design and optimization of the dehydrogenation–hydrogenation reaction of potential liquid organic hydrogen carriers.

Supplementary Information The online version contains supplementary material available at https://doi.org/10.1007/s11144-021-02037-1.

Acknowledgements The research was supported by the Russian Federation Government, Resolution No. 220, Grant No. 14.Z50.31.0038.

Declarations

Conflict of interest The authors declare that they have no known competing financial interests or personal relationships that could have appeared to influence the work reported in this paper.

References

1. Abdin Z, Zafaranloo A, Rafiee A, Merida W, Lipinski W, Khalilpour KR (2020) Hydrogen as an energy vector. Renew Sustain Energy Rev 120:109620. https://doi.org/10.1016/j.rser.2019.109620
2. Avci Hansu T, Sahin O, Caglar A, Kivrak H (2020) A remarkable Mo doped Ru catalyst for hydrogen generation from sodium borohydride: the effect of Mo addition and estimation of kinetic parameters. Reac Kinet Mech Cat 131:661–676. https://doi.org/10.1007/s11144-020-01884-8
3. Avci Hansu T, Sahin O, Caglar A, Kivrak H (2021) Untangling the cobalt promotion role for ruthenium in sodium borohydride dehydrogenation with multiwalled carbon nanotube-supported binary ruthenium cobalt catalyst. Int J Energy Res 45(4):6054–6066. https://doi.org/10.1002/er.6226
4. Preuster P, Papp C, Wasserscheid P (2017) Liquid organic hydrogen carriers (LOHCs): Toward a hydrogen-free hydrogen economy. Acc Chem Res 50:74–85. https://doi.org/10.1021/acs.accounts.6b00474
5. Niermann M, Dru S, Kaltschmitt M, Bonhoff K (2019) Environmental Science techno-economic analysis of LOHCs in a defined process chain. Energy Environ Sci 12:290–307. https://doi.org/10.1039/c8ee02700e
6. Jiang Z, Pan Q, Xu J, Fang T (2014) Current situation and prospect of hydrogen storage technology with new organic liquid. Int J Hydrogen Energy 39:17442–17451. https://doi.org/10.1016/j.ijhydene.2014.01.199
7. Klvana D, Chaouki J, Kusohorsky D, Chavarie C, Pajonk GM (1988) Catalytic storage of hydrogen: Hydrogenation of toluene over a nickel/silica aerogel catalyst in integral flow conditions. Appl Catal 42:121–130. https://doi.org/10.1016/S0166-9834(00)80080-9
8. Kalenchuk AN, Bogdan VI, Dunaev SF, Kustov LM (2018) Dehydrogenation of polycyclic naphthenes on a Pt/C catalyst for hydrogen storage in liquid organic hydrogen carriers. Fuel Process Technol 169:94–100. https://doi.org/10.1016/j.fuproc.2017.09.023
9. Muller K, Stark K, Emel'yanenko VN, Varfolomeev MA, Zaitsau DH, Shoifet E, Schick C, Verevkin SP, Arlt W (2015) Liquid organic hydrogen carriers: thermophysical and thermochemical studies of benzyl- and dibenzyl-toluene derivatives. Ind Eng Chem Res 54(32):7967–7976. https://doi.org/10.1021/acs.iecr.5b01840
10. Crabtree RH (2008) Hydrogen storage in liquid organic heterocycles. Energy Environ Sci 1:134–138. https://doi.org/10.1039/B805644G
11. Hodoshima S, Arai H, Takaiwa S, Saito Y (2003) Catalytic decalin dehydrogenation/naphthalene hydrogenation pair as a hydrogen source for fuel-cell vehicle. Int J Hydrogen Energy 28:1255–1262. https://doi.org/10.1016/S0360-3199(02)00250-1
12. Sebastián D, Bordejé EG, Calvillo L, Lázaro MJ, Moliner R (2008) Hydrogen storage by decalin dehydrogenation/naphthalene hydrogenation pair over platinum catalysts supported on activated carbon. Int J Hydrogen Energy 33:1329–1334. https://doi.org/10.1016/j.ijhydene.2007.12.037
13. Ninomiya W, Tanabe Y, Sotowa KI, Yasukawa T, Sugiyama S (2008) Dehydrogenation of cycloalkanes over noble metal catalysts supported on active carbon. Res Chem Intermed 34:663–668. https://doi.org/10.1163/156856708786189267
14. Tien PD, Satoh T, Miura M, Nomura M (2005) Efficient and reusable palladium catalysts supported on activated carbon fibers for dehydrogenation of tetrahydronaphthalene. Energy Fuels 19(3):731–735. https://doi.org/10.1021/ef040083v
15. Kalenchuk AN, Smetneva DN, Bogdan VI, Kustov LM (2015) Kinetics of decalin dehydrogenation on Pt/C catalyst. Russ Chem Bull 64:2642–2645. https://doi.org/10.1007/s11172-015-1202-1
16. Lee G, Jeong Y, Kim BG, Han JS, Jeong H, Na HB, Jung JC (2015) Hydrogen production by catalytic decalin dehydrogenation over carbon-supported platinum catalyst: effect of catalyst preparation method. Catal Commun 67:40–44. https://doi.org/10.1016/j.catcom.2015.04.002
17. Shinohara C, Kawakami S, Moriga T, Hayashi H (2004) Local structure around platinum in Pt/C catalysts employed for liquid-phase dehydrogenation of decalin in the liquid-film state under reactive distillation conditions. Appl Catal 266:251–255. https://doi.org/10.1016/j.apcata.2004.02.014
18. Dokjampa S, Rirksomboon T, Osuwan S, Jongpatiwut S, Resasco DE (2007) Comparative study of the hydrogenation of tetralin on supported Ni, Pt, and Pd catalysts. Catal Today 123:218–223. https://doi.org/10.1016/j.cattod.2007.01.004
19. Dziewiecki Z, Ihnatowicz M, Makowski A (1979) Activity of Ni-Moly catalysts in tetralin or decalin dehydrogenation and in hydrogenation of coal-extract solution. Fuel 58:737–740. https://doi.org/10.1016/0016-2361(79)90072-3

20. Ninomiya W, Tanabe Y, Uehara Y, Sotowa K, Sugiyama S (2006) Dehydrogenation of tetralin on Pd/C and Te-Pd/C catalysts in the liquid-film state under distillation conditions. Catal Lett 110:191–194. https://doi.org/10.1007/s10562-006-0108-9
21. Tien PD, Satoh T, Miura M, Nomura M (2005) Continuous hydrogen evolution from tetrahydronaphthalene over palladium catalysts supported on activated carbon fibers. Energy Fuels 19(5):2110–2113. https://doi.org/10.1021/ef050090z
22. Kim K, Oh J, Kim TW, Park JH, Han JW, Suh YW (2017) Different catalytic behaviors of Pd and Pt metals in decalin dehydrogenation to naphthalene. Catal Sci Technol 7:3728–3735. https://doi.org/10.1039/c7cy00569e
23. McVicker G (2002) Selective ring opening of naphthenic molecules. J Catal 210:137–148. https://doi.org/10.1006/jcat.2002.3685
24. Martynenko E, Pimerzin AA, Savinov A, Pimerzin A, Verevkin S (2020) Hydrogen release from decalin by catalytic dehydrogenation over supported platinum catalysts. Top Catal 100:100. https://doi.org/10.1007/s11244-020-01228-9
25. Sun JM, Bao XH (2008) Textural manipulation of mesoporous materials for hosting of metallic nanocatalysts. Chem Eur J 14:7478–7488. https://doi.org/10.1002/chem.200800823
26. Zhao D, Huo Q, Feng J, Chmelka BF, Stucky GD (1998) Nonionic triblock and star diblock copolymer and oligomeric surfactant syntheses of highly ordered, hydrothermally stable, mesoporous silica structures. J Am Chem Soc 120:6024–6036. https://doi.org/10.1021/ja974025i
27. Schumacher K, Ravikovitch PI, Chesne AD, Neimark AV, Unger KK (2000) Characterization of MCM-48 materials. Langmuir 16(10):4648–4654. https://doi.org/10.1021/la991595i
28. Suttisawat Y, Horikoshi S, Sakai H, Abe M (2010) Hydrogen production from tetralin over microwave-accelerated Pt-supported activated carbon. Int J Hydrogen Energy 35:6179–6183. https://doi.org/10.1016/j.ijhydene.2010.03.086
29. Kruk M, Jaroniec M, Ko C, Ryoo R (2000) Characterization of the porous structure of SBA-15 supporting information. Chem Mater 12:1961–1968. https://doi.org/10.1021/cm000164e
30. Zhang K, Yuan EH, Xu LL, Xue QS, Luo C, Albela B, Bonneviot L (2012) Preparation of high-quality MCM-48 mesoporous silica and the mode of action of the template. Eur J Inorg Chem. https://doi.org/10.1002/ejic.201200316
31. Ortega-Domínguez RA, Vargas-Villagrán H, Peñaloza-Orta C, Saavedra-Rubio K, Bokhimi X, Klimova TE (2017) A facile method to increase metal dispersion and hydrogenation activity of Ni/SBA-15 catalysts. Fuel 198:110–122. https://doi.org/10.1016/j.fuel.2016.12.037
32. Wei FY, Liu ZW, Lu J, Liu ZT (2010) Synthesis of mesoporous MCM-48 using fumed silica and mixed surfactants. Microporous Mesoporous Mater 131:224–229. https://doi.org/10.1016/j.micromeso.2009.12.027
33. Souza MJB, Garrido Pedrosa AM, Cecilia JA, Gil-Mora AM, Rodríguez-Castellón E (2015) Hydrodesulfurization of dibenzothiophene over PtMo/MCM-48 catalysts. Catal Commun 69:217–222. https://doi.org/10.1016/j.catcom.2015.07.004
34. Ichikawa S, Poppa H, Boudart M (1985) Disproportionation of CO on small particles of silica-supported palladium. J Catal 91(1):1–10. https://doi.org/10.1016/0021-9517(85)90282-9
35. Wang B, Goodman DW, Froment GF (2008) Kinetic modeling of pure hydrogen production from decalin. J Catal 253:229–238. https://doi.org/10.1016/j.jcat.2007.11.012
36. Ritchie AW, Nixon AC (1970) Dehydrogenation of dicyclohexyl over a platinum-alumina catalyst without added hydrogen. Ind Eng Chem Prod Res Dev 9:213–219. https://doi.org/10.1021/i360034a019
37. Dutta RP, Schobert HH (1996) Hydrogenation/dehydrogenation of polycyclic aromatic hydrocarbons using ammonium tetrathiomolybdate as catalyst precursor. Catal Today 31:65–77. https://doi.org/10.1016/0920-5861(96)00084-3

Publisher's Note Springer Nature remains neutral with regard to jurisdictional claims in published maps and institutional affiliations.

Authors and Affiliations

Evgeniya A. Martynenko[1] · **Sergei V. Vostrikov**[1] · **Aleksey A. Pimerzin**[1]

✉ Evgeniya A. Martynenko
martynenko.ea@samgtu.ru

[1] Samara State Technical University, Molodogvardeyskaya st. 244, Samara, Russia 443100